Is the outcrop topology of dolerite dikes of the Precambrian Singhbhum Craton fractal?

Nibir Mandal[1], Atin Kumar Mitra[1], Santanu Misra[1] and Chandan Chakraborty[2,*]

[1] *Department of Geological Sciences, Jadavpur University, Kolkata 700 032, India.*
[2] *Geological Studies Unit, Indian Statistical Institute, 203, B. T. Road, Kolkata 700 108, India.*
[*] *e-mail: chandan@isical.ac.in*

In the Precambrian Singhbhum Craton of eastern India, newer dolerite dikes occur profusely with varying outcrop lengths. We have analysed the nature of their length-size and orientation distributions in relation to the theory of fractals. Two orientational sets of dikes (NW–SE and NE–SW) are present. Both the sets show strongly non-power-law size distributions, as reflected in non-linear variations in logarithmic space. We analyzed thousands of data, revealing that polynomial functions with a degree of 3 to 4 are the best representatives of the non-linear variations. Orientation analysis shows that the degree of dispersions from the mean trend tends to decrease with increasing dike length. The length-size distributions were studied by simulating fractures in physical models. Experimental fractures also show a non-power-law distribution, which grossly conforms to those of the dolerite dikes. This type of complex size distributions results from the combined effects of nucleation, propagation and coalescence of fractures.

1. Introduction

In recent times the concept of fractal geometry has been widely used in the analysis of geological objects in different scales, from river systems at map scale to sedimentary pores at micro-scale. The basic tenet of fractals employed in geological studies is mainly concerned with a power-law distribution of the object properties. For example, the number of rivers belonging to a certain order can be shown to vary with their wavelength following a power-law function (Korvin 1992). Such a distribution implies that the two parameters will have a linear variation in log space, where the gradient of the linear variation indicates the fractal dimension.

Fractal analysis has been employed to characterize the nature of fracture or fault populations in many tectonic belts (Walsh *et al* 1991; Watterson *et al* 1996; Jackson and Sanderson 1992; Turcotte 1992; Cowie *et al* 1993; Clark and Cox 1996; Wojtal 1996; Yielding *et al* 1996). Several workers have analyzed displacements on faults using the fractal theory, and demonstrated power-law variations with their length (Marrett and Allemendinger 1991; Cowie and Scholz 1992; Walsh and Watterson 1992; Villemin *et al* 1995; Clark and Cox 1996; Knot *et al* 1996; Gross *et al* 1997; Poulimenos 2000; Van Dijk *et al* 2000; Volland and Kruhl 2004). Similar analyses have been employed to estimate various geological parameters, e.g., hydraulic conductivity in jointed rocks (see Korvin 1992 and references therein). Some field and experimental studies reveal that fault-size distribution may not exactly follow a power-law function (Cladouhos and Marrett 1996; Nicol *et al* 1996; Basu 1996; Cello 1997; Klausen 2004), and depending on the fault growth process, the distributions can switch over to an exponential law function (Ackermann *et al* 2001). Theoretical analyses show that different parameters, e.g., finite net slip in case of faults or the opening in case of tensile fractures, are proportional to fracture dimensions. Understandably, these fracture-associated parameters are

Keywords. Dike; fractal geometry; fracture; Singhbhum Craton; size-distribution; power law; physical model.

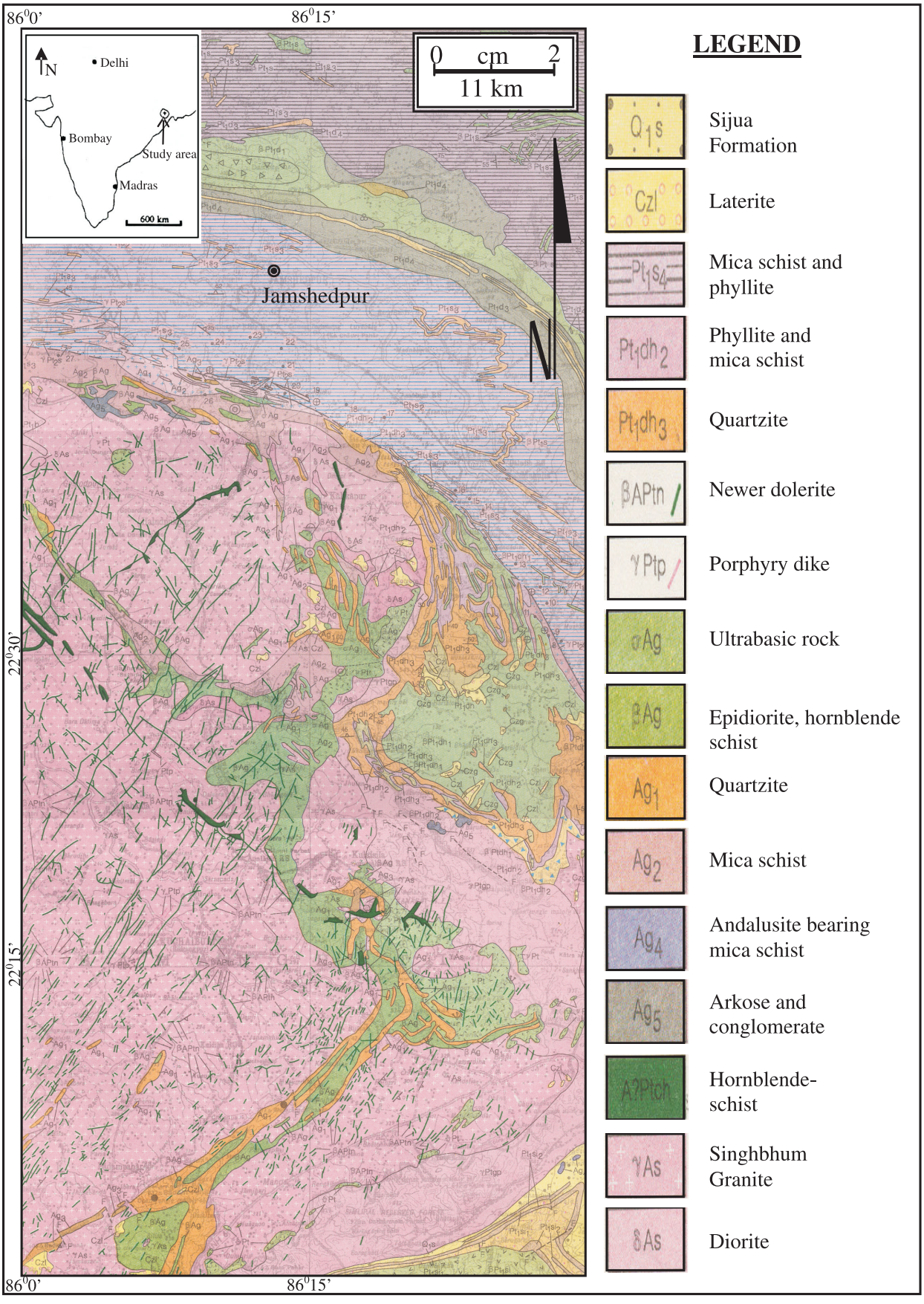

Figure 1. Geological map of the southern part of the Singhbhum Craton. (This is based on Map No 73J, Geological Survey of India). Note the profuse dolerite dikes (dark green) broadly forming two sets, trending NW–SE and NE–SW.

Figure 2. Dike hosted in metasedimentary rock in Ghatsila, Singhbhum region. The dike runs diagonally from top left to bottom right.

likely to show non-power law distributions (e.g. Gudmundsson 2004; Klausen 2004). In spite of significant developments in this subject over a couple of decades, further studies are needed for a better understanding of the geological factors controlling the fractal and non-fractal distribution of fractures or faults in natural systems.

We studied the geometrical distribution of newer dolerite dikes of the Precambrian Singhbhum Craton (figures 1, 2, Mukhopadhyay 2001 and references therein). The dikes define broadly two directional sets, trending NW–SE and NE–SW (figures 1, 3). Tectonic models demonstrate that the dikes have been emplaced along planes of disruption during early to late Proterozoic time (Dunn 1929; Dunn and Dey 1942; Sarkar 1984; Saha 1994; Gupta and Basu 2000; Mukhopadhyay 2001), which appear as conjugate shear fractures. In this paper we analyze the nature of size distribution of these fracture systems. Dike lengths were measured from the published map of the Geological Survey of India (1996). We also considered their orientations, and analyzed them as a function of their length. In order to complement the field data, fractures were simulated in physical models. The size distributions of both the field and experimental fractures show systematic patterns inconsistent with those of power-law distributions.

2. Types of fractures

The Singhbhum Craton underwent brittle deformation, developing fractures of varying lengths, which acted as locales for emplacement of dikes (∼934 Ma; Sarkar and Saha 1962; Mukhopadhyay 2001). In this section we briefly review the different types of fractures, in particular those filled by dolerite dikes. Experimental and field observations show that brittle deformation of rocks can occur

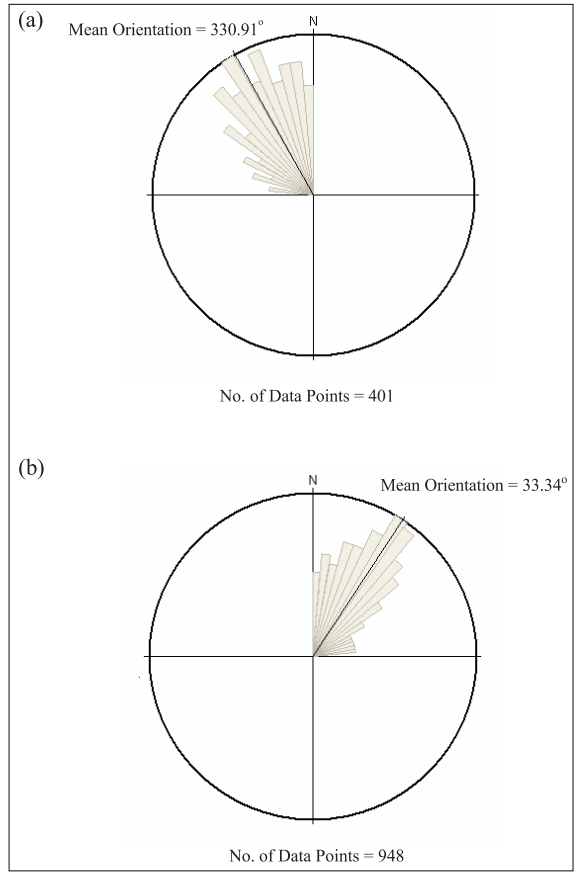

Figure 3. Rose diagram showing two populations of dikes **(a)** NW trending dikes and **(b)** NE trending dikes. Dark line indicates the vector mean of each population.

in two principal types: tensile fracturing and shear fracturing (Jager 1969; Ranalli 1987). In the latter type, the slip direction may be parallel or perpendicular to the tip line of fractures (Atkinson 1987). These are two end-member types, and there can be fracturing by a combination of extension and shear, described as extensional shear or hybrid fracturing (figure 4). There are several physical factors that govern the mode of fracturing. One of the important factors is confining pressure. It has been observed in experiments that increasing pressure generally leads to a transition from the tensile to the shear mode of failure (Griggs and Handin 1960; Paterson 1978). There are other physical factors controlling the nature of fracturing in rocks. For example, in layered systems the mode of fracturing depends on the thickness ratio of competent and incompetent layers (Mandal *et al* 2000).

The orientation of fractures depends essentially on the principal axes of stress. Tensile fractures form parallel to the principal compression direction and perpendicular to the principal tension direction. On the other hand, shear fractures develop parallel to the intermediate principal axis of stress,

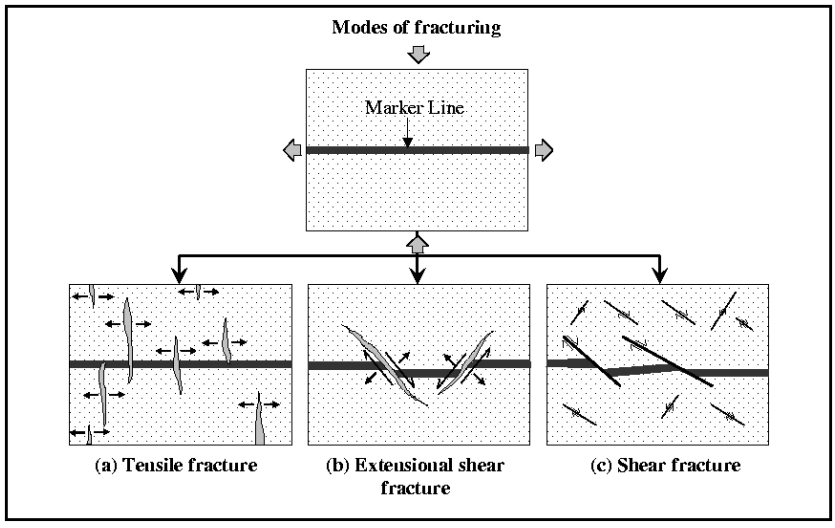

Figure 4. Three principal modes of fracturing. **(a)** Tensile fracturing, **(b)** Extensional shear fracturing and **(c)** Shear fracturing. Dark band is shown as a marker for revealing the nature of displacement across the fractures. This is a sectional view perpendicular to the intermediate axis of principal stress.

and usually make an angle less than 45° with the principal compression direction (figure 5). Under tectonic compressive stresses shear fractures generally develop in conjugate sets. The line of intersection between the two sets is along the intermediate stress axis, which is vertical. The overall geometry of fracture patterns in the Singhbhum Craton resembles conjugate shear fractures, and appears to have developed in response to a horizontal N–S compressive stress, maintaining the intermediate stress axis nearly vertical. The fractures show a wide variation in their strike trace length, ranging a few metres to several kilometres (table 1). This variation gives an impression of self-similarity in their pattern. The following sections present an analysis of their size distributions.

3. Size distribution of dolerite dikes

3.1 *Method of analysis*

We analyzed the size distribution of dolerite dikes considering them as one-dimensional objects. Mandelbrot (1967) had shown for the first time that objects forming a fractal set follow:

$$N_n = C\frac{1}{r_n^D}, \qquad (1)$$

where N_n is the number of objects (i.e., fragments) with a characteristic linear dimension r_n and C is a constant of proportionality, and D is the fractal dimension (Turcotte 1992). A fractal dimension may be an integer, which is equivalent to Euclidean dimension. For example, the Euclidean dimensions of a point, a line, a square and a cube are 0, 1, 2 and 3 respectively. On the other hand, the fractal dimension is not an integer but a fraction (Turcotte 1992).

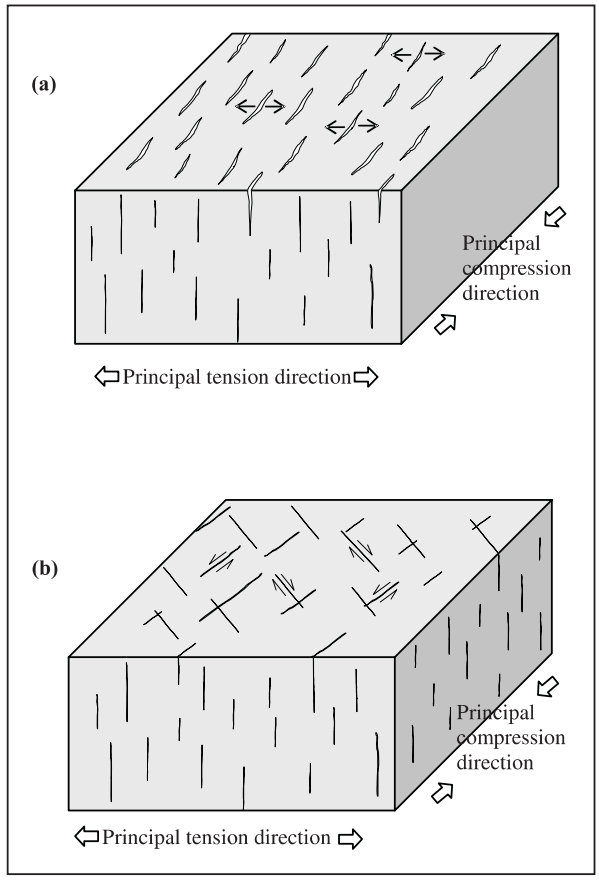

Figure 5. Geometrical dispositions of tension **(a)** and shear **(b)** fractures in relation to the principal axes of stress.

Table 1. *Frequency distribution of newer dolerite dikes in Precambrian Singhbhum Craton.*

Length of dikes (×250 m)	No. of dikes
Frequency distribution of NW trending dikes	
>0.5–1.5	92
>1.5–2.5	132
>2.5–3.5	58
>3.5–4.5	30
>4.5–5.5	32
>5.5–6.5	22
>6.5–7.5	7
>7.5–8.5	7
>8.5–9.5	3
>9.5–10.5	5
>10.5–11.5	2
>11.5–12.5	3
>12.5–13.5	1
>13.5–14.5	0
>14.5–15.5	2
>15.5–16.5	1
>16.5–18.5	0
>18.5–19.5	2
>19.5–22.5	0
>22.5–23.5	1
>23.5–28.5	0
>28.5–29	1
Frequency distribution of NE trending dikes	
>0.5–1.5	138
>1.5–2.5	354
>2.5–3.5	144
>3.5–4.5	88
>4.5–5.5	57
>5.5–6.5	43
>6.5–7.5	23
>7.5–8.5	14
>8.5–9.5	19
>9.5–10.5	17
>10.5–11.5	9
>11.5–12.5	6
>12.5–13.5	8
>13.5–14.5	3
>14.5–15.5	4
>15.5–16.5	2
>16.5–17.5	2
>17.5–18.5	0
>18.5–19.5	2
>19.5–20.5	1
>20.5–21.5	2
>21.5–22.5	1
>22.5–23.5	0
>23.5–24.5	3
>24.5–25.5	1
>25.5–26.5	0
>26.5–27.5	2
>27.5–32.5	0
>32.5–33.5	1
>33.5–34.5	1
>34.5–35.5	2
>35.5–36.5	1

Equation (1) can also be written in the form:

$$\ln N_n = \ln C - D \ln r_n, \tag{2}$$

$$Y = K - DX, \tag{3}$$

where $Y = \ln N_n$ and $X = \ln r_n$. Equation (2b) shows that the number of objects and their length will have a linear variation when plotted in the XY space, where X and Y are the log values of the parameters under consideration. Data with a power-law variation will thus be characterized by a linear distribution in the log space.

In our case we deal with dike length (X) and the number of dikes (Y) of a characteristic length as the parameters for our analysis (table 1), and attempt to reveal if their distributions, apparently self-similar in look, do obey the rule of fractal (equation 1). We used the published map of GSI (1996) in the scale: 1 cm = 2.5 km (figure 1). It may be noted that the fractures show traces on a section nearly perpendicular to the intermediate principal axis of stress and parallel to the movement direction. This provides us a good opportunity to deal with actual length of the fractures, showing a strike-slip movement. We consider the dispositions of dikes shown in the geological map of GSI reliable, as they have been traced out based on ground observations. Secondly, the terrain is mostly granitic, and the ground surface is almost flat (Topographic sheet no. 73/J, Survey of India), and the outcrop pattern is not affected by topography. Dikes in the two populations (NW–SE and NE–SW; figure 3) are mostly steeply dipping, and therefore the distributions observed at the present level of erosion are likely to remain statistically similar with varying sectional levels.

Dike lengths and orientations were determined from their traces on the quadrangle geological map (figure 6). Most of the dikes show reasonably straight trajectories (figure 6a). To measure the length of dikes with minute irregularities, a straight line was drawn along the mean trend of the dike, and the length of the dike was measured along that straight line (figure 6b). Some of

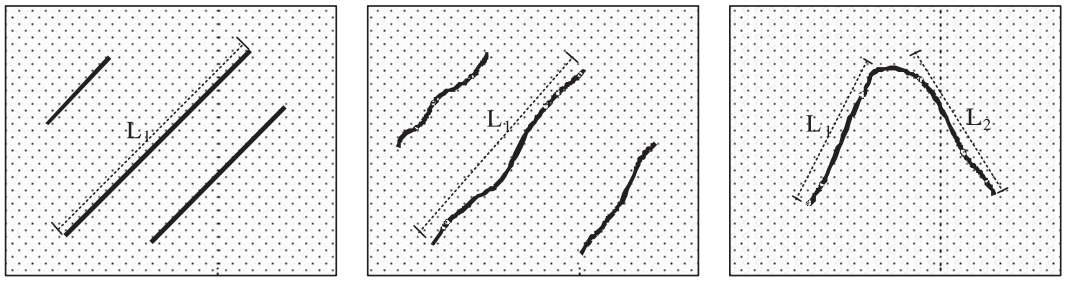

Figure 6. Measurements of length of dikes with different geometry; **(a)** straight dikes, **(b)** dikes with slight geometrical irregularities. Dashed line shows length along the mean trend and **(c)** two differently oriented dikes coalescing each other. In this case their lengths are measured separately.

the dikes show tangled geometry, similar to dislocations observed in defect crystals. They actually represent coalescence of two dikes of different orientations. We measured their length and orientation independently (figure 6c). The analyses of the two populations of dikes are presented in the following sections.

3.2 *NW–SE trending dikes*

The NW–SE trending dikes show a wide variation in their length (table 1). We plotted the dike lengths and their numbers in the XY space (figure 7a). The data show a systematic variation, but their regression follows a trend with a strong departure from linearity as reflected in the increase in R^2 value with increasing degree of polynomial order (figure 7a–e). The non-linearity in the XY space indicates that the NW–SE trending dikes do not follow a fractal distribution, though they apparently do so in the map (figure 1). It may be noted that different kinematic parameters of fractures, such as opening or slip, are found to be proportional to their length dimension (Li 1987; Pollard and Segall 1987; Vermyli and Scholz 1995; Gudmundsson 2000). Thus, other geometrical parameters, such as dike thickness are likely to have similar non-fractal distributions, as documented from several field observations (e.g., Gudmundsson 2004; Klausen 2004).

We have analyzed the length-size distribution considering best-fit polynomial curves of different degrees. If a straight line is chosen, data points show departures on the positive side in the lower size fraction, whereas negative departures in the higher size fraction (figures 7a–b). Increasing the polynomial degree to 2, the best-fit curve shows a slight curvature with convexity in the positive direction (figure 7c). However, data points still show large departures from the overall trend ($R^2 = 0.9182$). With further increase in the polynomial degree to 3, the best-fit curve is obtained, which shows a reasonably good match with the data points ($R^2 = 0.9658$; figure 7d). The geometry of the curve does not change much when the polynomial degree is increased to 4 ($R^2 = 0.966$; figure 7e). The curve is sigmoidal in shape, where its flanks show relatively gentle gradients. It appears from the curve that the distribution in middle-size range has a tendency to follow a more or less a straight trend line. Considering this size range (1 to about 2.5 in the log space; figure 7), the distribution can be approximated as fractal. However, the overall distribution does not strictly follow the power-law.

In summary, NW–SE trending dolerite dikes do not follow a fractal distribution. In contrast, a polynomial function with a degree of 3 ($R^2 = 0.9658$) or more is a better approximation for size distribution in the log space.

3.3 *NE–SW trending dikes*

In the same way we analyzed the size distribution of NE–SW trending dikes. The dispersion of data points in the XY space was somewhat more scattered than the NW–SE trending dikes, though are confined within a lower and an upper bound (figure 8a).

Generally, the data points show a strong departure from a straight line, implying a non-fractal size distribution (figure 8b). Increasing the polynomial degree to 2, the curve does not fit well with the data points (figure 8c), as in the previous case. The polynomial curve shows a strong curvature with the concave side facing up. The degree of match betters with increasing polynomial order (figure 8d). For a polynomial degree of 4, a better match ($R^2 = 0.7802$) is obtained, where the curve describes typically a sigmoidal shape (figure 8e), which is similar to that obtained for NW–SE trending dikes. The flanks of the curves show relatively gentle gradients.

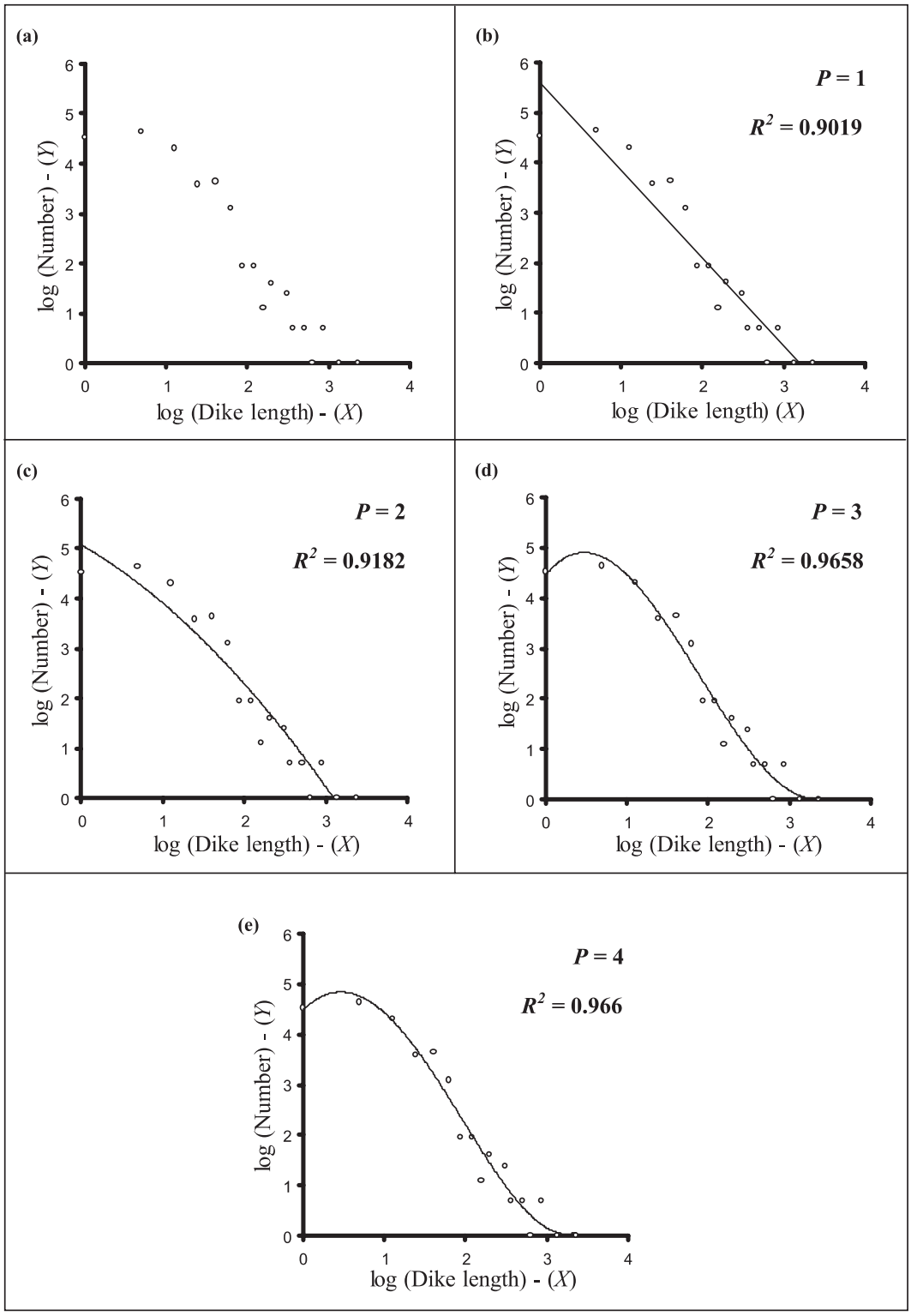

Figure 7. **(a)** Length (X) versus number (Y) plots in a logarithmic space for NW-trending dikes. **(b)**–**(e)** Extrapolation of the best fitting curve to the data by increasing polynomial degree (P).

3.4 *Interpretation of field data*

The size distributions of both NW–SE and NE–SW trending dolerite dikes are clearly non-fractal in nature, and show strong departures from the power-law distributions (cf. Ackermann *et al* 2001; Klausen 2004). Let us first inspect the nature of these departures, and then analyze the non-fractal distributions in the light of fracture mechanics. Based on the distribution (polynomial function of

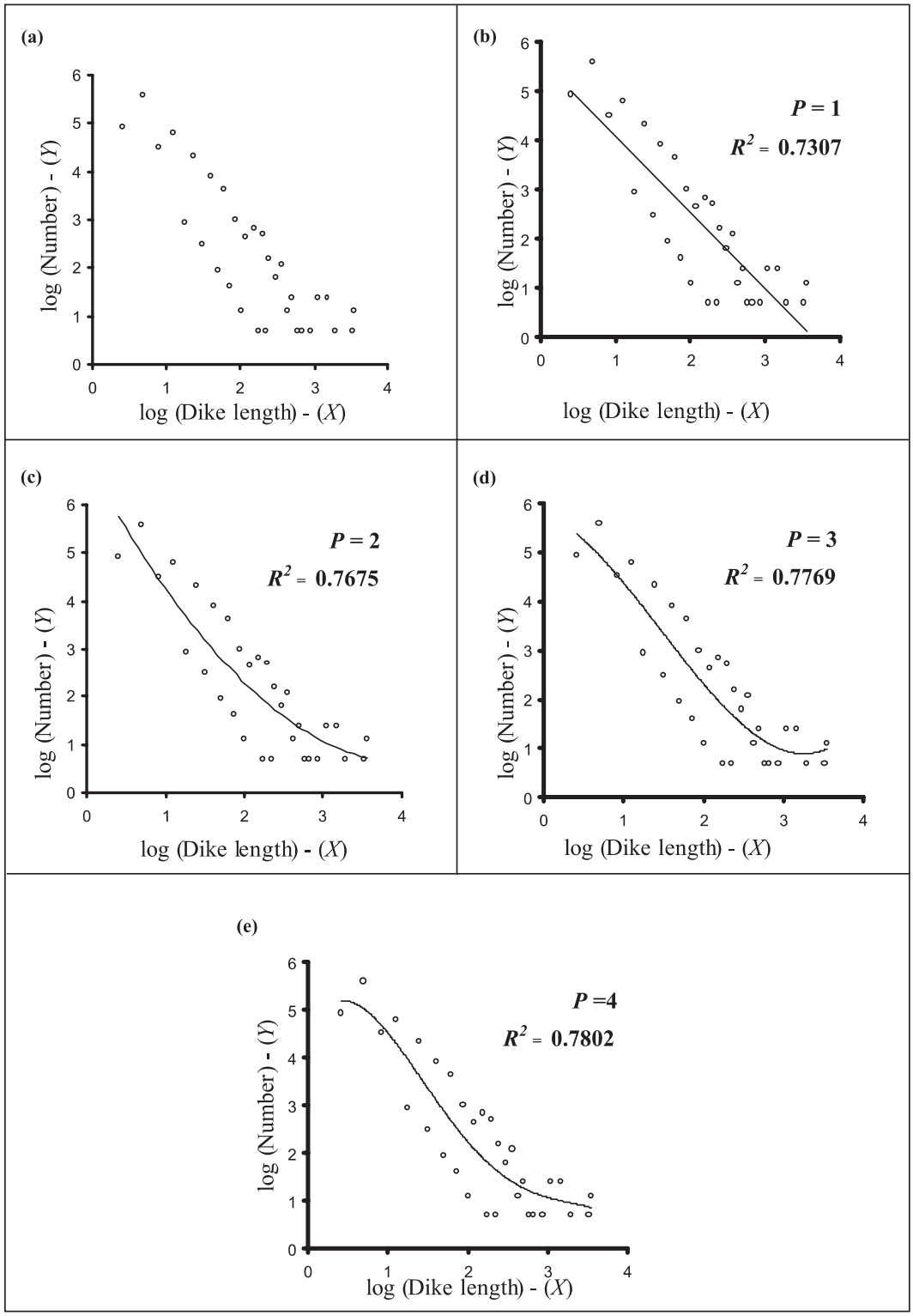

Figure 8. **(a)** Length (X) versus number (Y) plots in a logarithmic space for NE-trending dikes. **(b)**–**(e)** Extrapolation of the best fitting curve to the data by increasing polynomial degree (P).

degree 3–4), we consider an ideal curve in the XY space (figure 9), and take a tangent line at the point of inflection of the polynomial curve. The size-distribution would follow the tangent line if the dikes were ideally fractal in their size distribution. The polynomial curve is deflected downward from the tangent line for the smaller size range. This departure implies that the number of dikes of smaller lengths is less than that predicted from the power-law distribution. On the

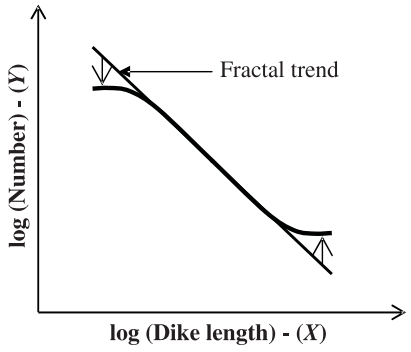

Figure 9. Idealized curve showing the variation of dike length and their corresponding number in a log space. Thin line represents the probable fractal trend of the size population (the line is drawn tangentially at the point of inflection).

other end, the curve shows upward deflection from the tangent line, indicating longer dikes larger in number than that predicted from the ideal size distribution.

In order to interpret these departures, we consider the process of fracture development in rocks. There are three processes involved in the evolution of fractures:

(1) nucleation of fractures,
(2) propagation of fractures and
(3) coalescence of fractures in the course of their propagation (figure 10).

These three processes operate simultaneously, but at different rates in successive stages of brittle deformation. For example, nucleation of fractures is likely to dominate at the initial stage, the rate of which is likely to reduce with progressive deformation (cf. Ackermann *et al* 2001), as the nucleation of fractures will be associated with a stress drop in their surroundings (Pollard and Segall 1981; Ji *et al* 1997). On the other hand, coalescence of fractures will be progressively more active in the course of brittle deformation.

We now try to extrapolate the conditions developing fractures with a power-law size distribution. Consider a system of fractures uniformly distributed in a physical space. Following the reverse process of fragmentation, the fractures can be linked randomly to produce fractures of increasing lengths. At any moment of progressive development of the fracture system, the length size distribution is likely to follow a power-law size distribution. This distribution is likely to be perturbed as soon as the effects of nucleation of new fractures or increases in fracture lengths due to propagation are added to the system. If the

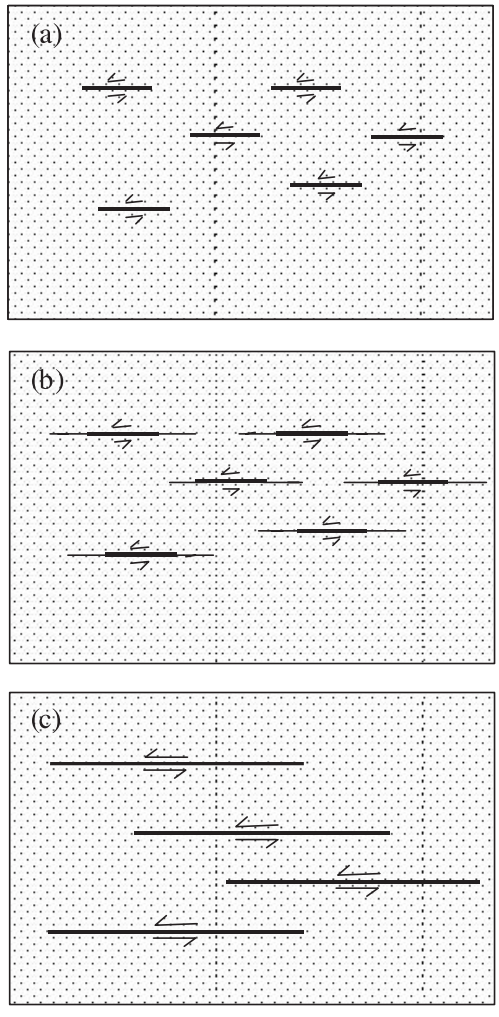

Figure 10. Successive stages of development of a fracture system involving three principal processes: **(a)** nucleation of fractures, **(b)** propagation of fractures and **(c)** coalescence of fractures.

fractures coalesce and at the same time propagate in length, the resultant lengths of fractures will be larger than these predicted from the process of coalescence only. This explains the polynomial size distributions with long dikes being more in number. On the other hand, it is somewhat difficult to explain why fractures of smaller length are less in number, compared to the power-law size distribution. We infer that, following nucleation fractures immediately propagate, and increase in length. Secondly, nucleation of new fractures would produce fractures of smaller size, maintaining the size distribution as expected in fractal distribution. However, the nucleation rate of fractures is likely to be reduced with progressive deformation. As a result, at the advanced stage, frequency of fractures of smaller lengths remain relatively less than that predicted by the power-law as also revealed from the field data (figure 7).

Table 2. *Variation of orientation for the different length classes of dikes.*

Length of dikes (×250 m)	Orientation of the dikes (in degrees)
Length versus orientation of NW–SE trending dikes	
>0.5–1.5	275–360
>1.5–2.5	276–360
>2.5–3.5	280–356
>3.5–4.5	300–359
>4.5–5.5	307–360
>5.5–6.5	290–357
>6.5–7.5	319–360
>7.5–8.5	292–354
>8.5–9.5	326–345
>9.5–10.5	307–357
>10.5–11.5	301–355
>11.5–12.5	321.5–338
>12.5–13.5	355
>13.5–14.5	–
>14.5–15.5	320–338
>15.5–16.5	325
>16.5–18.5	–
>18.5–19.5	316–324
>19.5–22.5	–
>22.5–23.5	335
>23.5–28.5	–
>28.5–29	308
Length versus orientation of NE–SW trending dikes	
>0.5–1.5	2–89
>1.5–2.5	2–82
>2.5–3.5	2–88
>3.5–4.5	2–88
>4.5–5.5	2–84
>5.5–6.5	3–86
>6.5–7.5	7–63
>7.5–8.5	5–45
>8.5–9.5	7–78
>9.5–10.5	6–85
>10.5–11.5	23–47
>11.5–12.5	4–37
>12.5–13.5	4–35
>13.5–14.5	7–36
>14.5–15.5	15–32
>15.5–16.5	3–35
>16.5–17.5	35–38
>17.5–18.5	–
>18.5–19.5	9–35
>19.5–20.5	25
>20.5–21.5	27–39
>21.5–22.5	14
>22.5–23.5	–
>23.5–24.5	30–38
>24.5–25.5	30
>25.5–26.5	–
>26.5–27.5	34–42
>27.5–32.5	–
>32.5–33.5	40
>33.5–34.5	37.5
>34.5–35.5	29–31
>35.5–36.5	38

4. Analysis of dike orientation

4.1 *Approach*

The orientations of individual dikes of both NW–SE and NE–SW trending sets show wide dispersion from the respective mean orientations (figure 3; table 2). In this section we analyze the orientation distribution of dikes as a function of their length. The orientations of dikes in each set were measured separately, and analyzed in two steps (figures 11, 12). First, the geographic orientations and the lengths of dikes were plotted in a Cartesian space. Such plots show a systematic variation in orientation dispersion with increasing dike length (figures 11, 12). In the second step, the degree of dispersion from the mean trend of dikes (θ_t; figure 3) is taken as a parameter (D). According to the concept, a parameter associated with fractal objects can be expressed as:

$$D = KL^n, \tag{4}$$

where K is a constant and n is the exponent of power-law distribution. L is the length dimension of object (dike length in our case). D is taken as a measure of orientation dispersion, which is defined in terms of the following equation:

$$D = |\theta_b - \theta_t|, \tag{5}$$

where θ_t is the observed value.

The purpose of our analysis is to investigate if the orientation dispersion (D) holds a power-law distribution with dike length (L), as defined in equation (3).

4.2 *NW–SE trending dikes*

The orientations of dikes show a wide variation, encompassing virtually the entire NW quadrant (figure 11a). However, they tend to attain a persistent orientation with increasing length, which is also apparent in the geological map (figure 1).

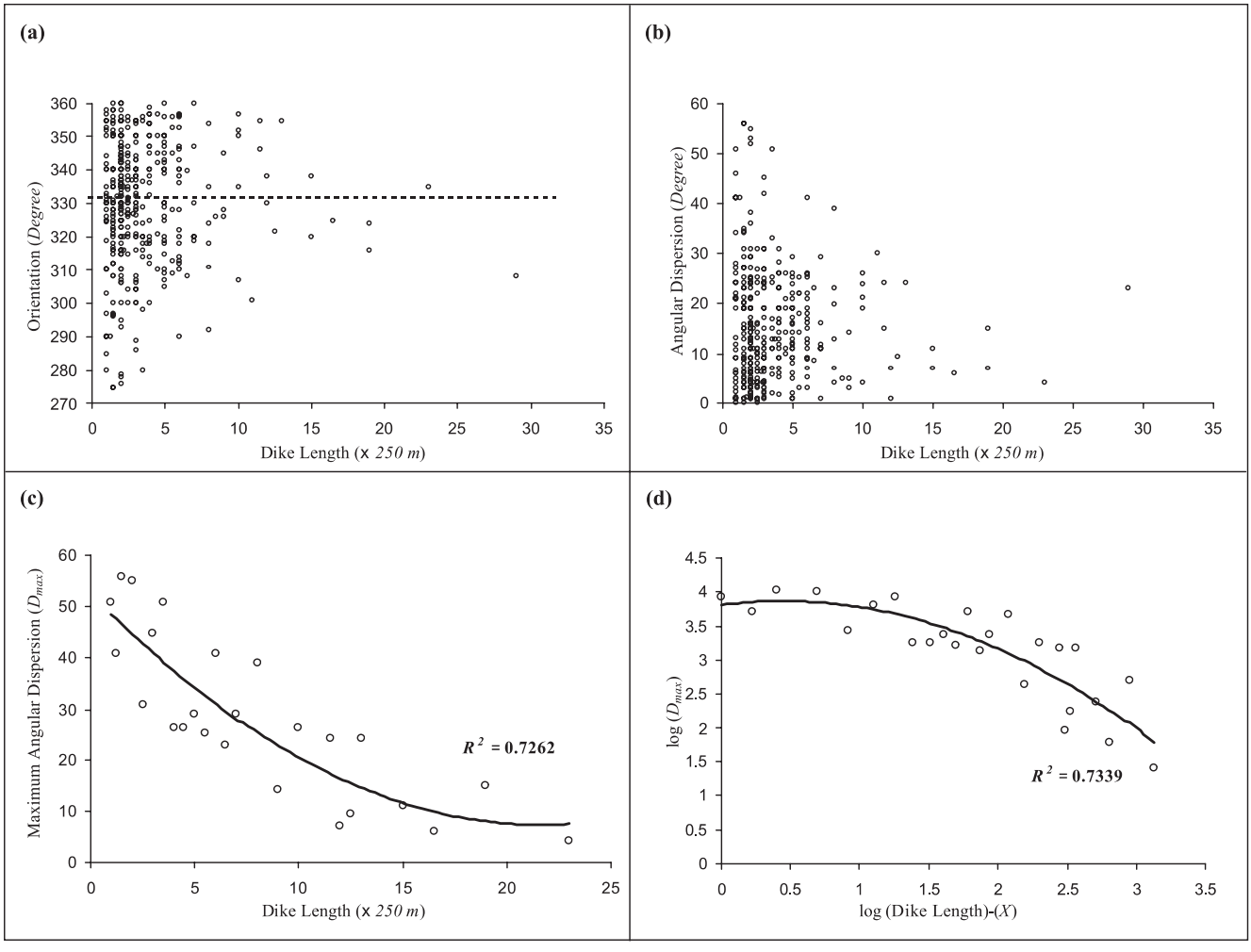

Figure 11. **(a)** Plot showing the variation in the orientation of NW trending dikes as a function of their length, **(b)** represent their dispersions from the mean trend as function of dike length, and **(d)** maximum dispersion values ($D_{\max}$) as function of dike length, which is represented in logarithmic space in **(c)**.

The plot suggests that fractures are likely to be diversely oriented when they are small in size. Longer fractures develop through coalescence and propagation. These two processes probably occur tracking the principal axes of stress, and thereby lead fractures to orient themselves along a particular direction, irrespective of their initial orientations.

Using equation (4) we have determined angular dispersions (D) for individual dike and plotted them against the length (figure 11b), the plot shows that the D value decreases systematically with increasing dike length. We also determined the maximum orientation dispersions ($D_{\max}$) for different dike lengths, and plotted them against the length (figure 11c). $D_{\max}$ varies systematically with dike length. The value of $D_{\max}$ decreases systematically with dike-length and eventually assumes a stable value. We then plotted $D_{\max}$ and dike length in log–log space to test whether they obey a power-law distribution (figure 11d). Our plots clearly reveal that fluctuations in the orientation of dikes do not follow such a distribution, as reflected from the strong non-linearity in the variation. Following the method described in section 3.2, it appears that a polynomial function of degree 3 fits better with the distribution.

4.3 *NE–SW trending dikes*

Dikes in this population also show similar variations in their orientations (figure 12a). Data dispersion is large for smaller dike lengths. Dikes tend to attend a stable orientation with increasing length. Dispersion in dike orientations was analyzed using equation (4) and plotted against dike length and the plot shows the same pattern as the plot for NW–SE trending dikes (figure 12b). We have also determined maximum dispersion ($D_{\max}$) and plotted them against the length which also shows a systematic variation (figure 12c). The log–log plot of $D_{\max}$ versus dike-length variation is evidently

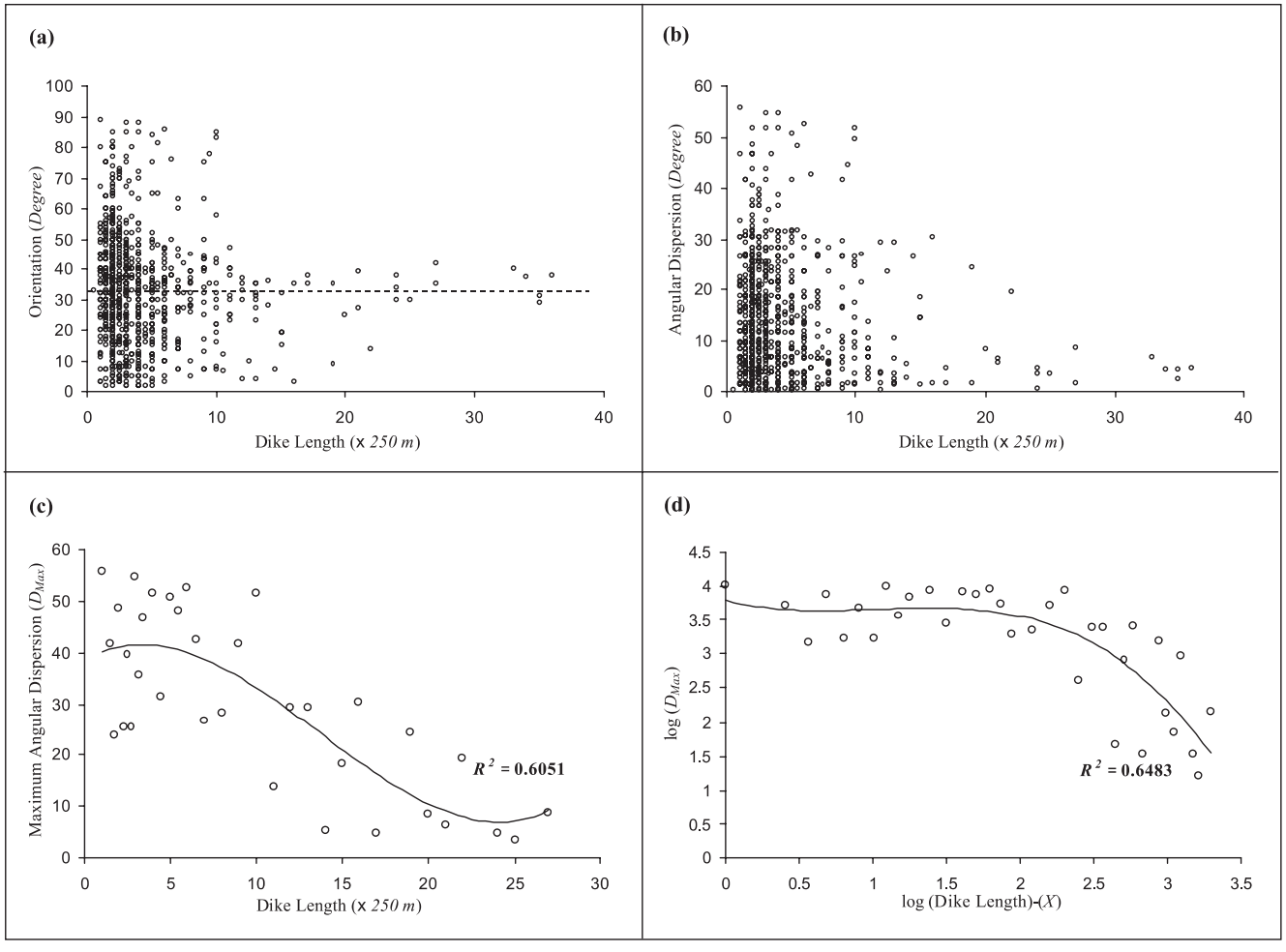

Figure 12. **(a)** Orientation distribution of NE trending dikes as a function of their length, **(b)** orientation dispersions of dikes with varying lengths, and **(c)** maximum dispersions values ($D_{\max}$) as a function of length, which is represented in logarithmic space in **(d)**.

non-linear, implying that the orientation dispersion of dikes does not follow a power-law function of their length (figure 12d). The nature of orientation distribution of NE–SW trending dikes is, however, grossly similar to that of NW–SE trending dikes.

5. Fracture-size population in physical models

5.1 *Experimental approach*

We simulated fractures in test models (cf. Mandal *et al* 1994). Experimental fractures were tensile in nature, instead of shear fractures discussed in the previous section. However, both tensile and shear fractures evolve in the same fashion, i.e., involving three principal processes: nucleation, propagation and coalescence, as discussed earlier. Experiments were performed by resting a brittle layer of plaster-of-paris on a viscous (pitch) block (figure 13). Brittle layer was developed in the following manner. A plastic sheet was placed on the pitch block. The plastic sheet had a rectangular blank area. Liquid plaster-of-paris was poured in the blank area in the form of a thin layer. The layer was allowed to dry for about 5 minutes. The plastic sheet was pulled out when the layer became somewhat dry. The tensile strength of the layer was measured to be 18.5×10^3 Pa. At this stage the pitch block was allowed to flow in horizontal direction under its own weight. The flow in the other horizontal direction was arrested by two glass plates. The viscous flow of pitch developed traction and thereby tensile stresses in the overlying layer. The entire setup was placed on glass plates, where the interfaces of all the glass plates, including the lateral and basal ones, were lubricated with liquid soap to minimize friction to flow in the pitch block.

The brittle layer underwent fracturing when the tensile stresses reached the tensile strength of plaster-of-paris. Successive stages of fracturing

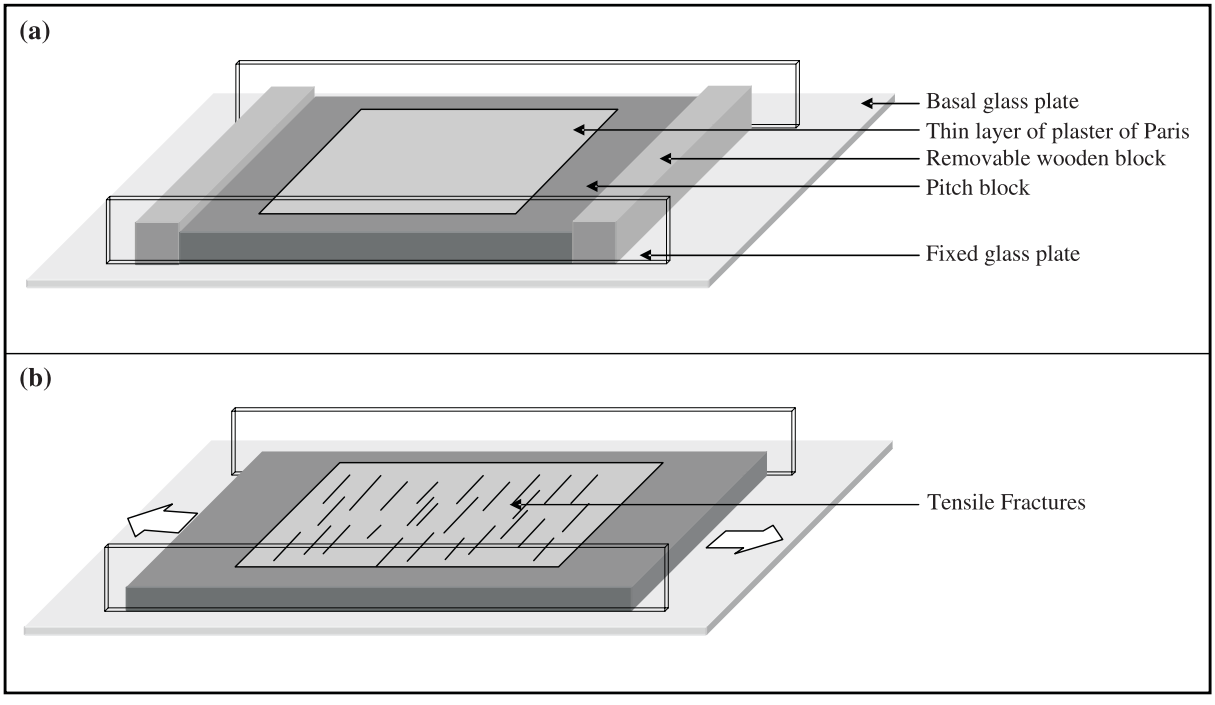

Figure 13. Experimental setup for simulation fractures in a brittle layer (plaster of paris). Arrows indicate the direction bulk flow in the model. **(a)** Initial model and **(b)** deformed model.

were photographed (figure 14). An analysis of experimental data is presented in the next section.

5.2 *Fracture-size distribution*

Following the method described in section 4, we plotted the number of fractures and their corresponding lengths in log space (figure 15a). The distribution was analyzed by increasing the order of polynomial function, as exercised for the dolerite dikes. Considering a straight line in the plot (figure 15b), it is revealed that the fracture-size distribution shows marked departures from a linear one, implying that the experimental fractures do not obey a fractal distribution. This type of non-fractal size distribution is consistent with that of newer dolerite dikes. By increasing the degree of polynomial, a better match is obtained as revealed from increasing R^2 values (figure 15). The data curve is gently convex up, which resembles that shown by the NW–SE trending dikes (figure 15c). However, there are still large departures of the data points from the curve of polynomial degree 2 ($R^2 = 0.5936$). The departures are minimized when the degree is increased to 3 ($R^2 = 0.6276$) (figure 15d). The distribution is represented by a curve of sigmoidal shape, which is also evident in the distribution of natural fracture systems (figure 7d).

We studied the different processes in the evolution of experimental fractures, which are illustrated in figure 16. At the initial stage a large number of cracks nucleated in the brittle layer. These cracks propagated as well as opened out and thereby produced fractures with lenticular shapes. At this stage further extension in the brittle layer produced new cracks, and earlier fractures propagated in length. Finally, coalescence of fractures became important. Our experimental results clearly reveal that fracture-size distributions are not likely to follow a power-law one, as the development of macro-scale fractures involve a combination of three processes: nucleation, propagation and coalescence.

6. Discussion

In Earth sciences a trend which looks into various geological systems in the light of fractal theory has been set over the last decade. A line of such work is concerned with understanding the nature of fracture populations and associated parameters, e.g., displacements. Power-law size distribution is a common type, where the number of faults varies linearly with the corresponding size in a log–log plot. However, several workers have reported non-linear distributions. There have not been many theoretical and experimental attempts for explaining the origin of non-fractal distributions. Based on our field observations and experimental findings, it seems that the fracture-size distribution is essentially controlled by the mode of fracture

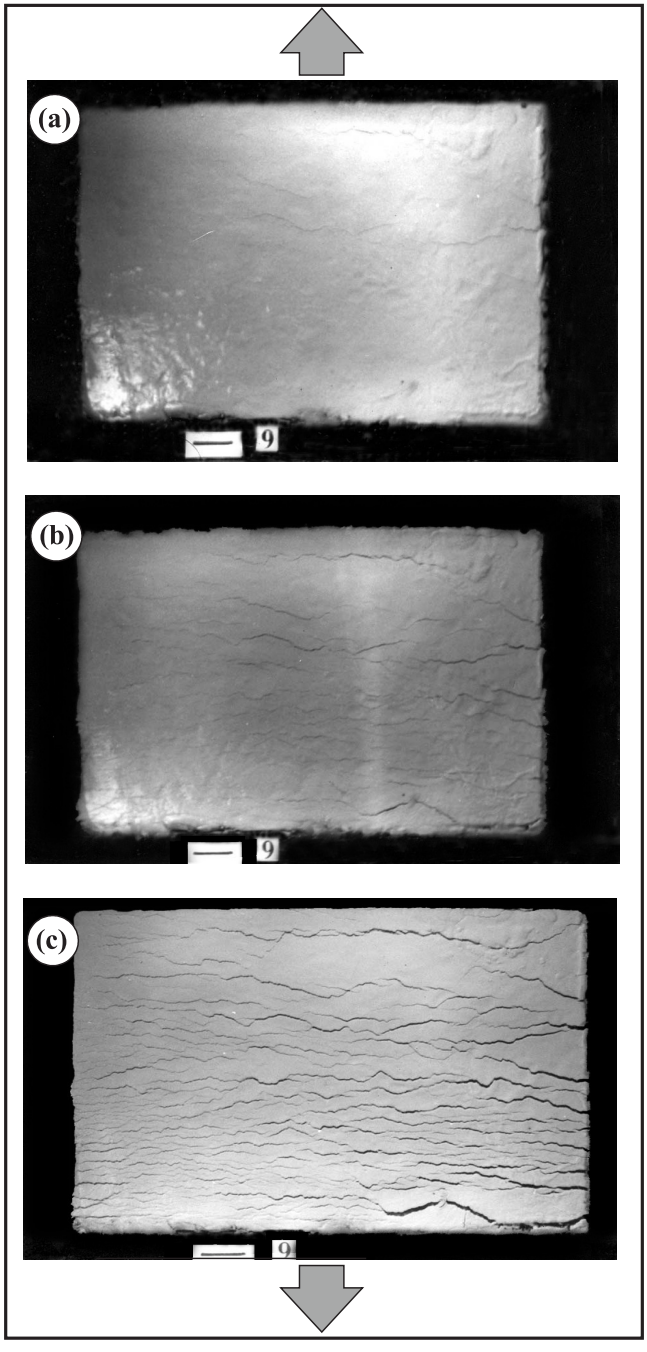

Figure 14. Successive stages of fracturing in a brittle layer under bulk extension (vertical direction).

growth (cf. Cladouhos and Marrett 1996). Most of the natural fracture populations involve the three processes of nucleation, propagation and coalescence of fractures. A population is likely to show non-power-law size distributions as these processes operate at varying rates. In order to quantify the size distribution of an evolving fracture population it is therefore necessary to understand the relative rates of the three processes, and how they can vary with time, giving a combined effect in the final size distribution.

Newer dolerite dikes in the Singhbhum Craton show non-linear distributions in log–log plots, which have not been reported earlier. The non-linearity is defined by polynomial functions with degrees 3 to 4, which also conform to that of experimental fractures. Non-power law distributions of fracture dimensions have been documented by several workers (Yielding *et al* 1996; Ackermann *et al* 2001; Gudmundsson 2004; Klausen 2004). It has been proposed that this kind of distribution may be a result of varying data resolutions or observational limitations (e.g., Yielding *et al* 1996). We performed physical experiments to address this issue, and noticed that the experimental fracture systems also showed a strong departure from a power-law distribution. The finding leads us to suggest that a fracture population can show a non-power law distribution even in an ideal situation. There are other probable factors, e.g., incompleteness in dike outcrops, which may have influenced the length distributions of the dike populations. To analyze this, consider a set of lines as an example. The lines are partially erased in a random fashion, which basically simulates a kind of fragmentation process. At any stage of this operation, line segments of varying lengths would tend to follow a power-law distribution (Turcotte 1992). Based on this point as well as experimental findings, we suggest that incompleteness in outcrop does not seem to be a crucial factor in dictating the distribution to follow a non-power law, as also suggested by others (Klausen 2004). An alternative model is thus presented to explain this type of size distribution qualitatively in terms of the three processes: nucleation, propagation and coalescence of fractures. However, the model describes schematically the mode of progressive evolution of a fracture system, and the approach is somewhat simplistic in nature. Evidently, the study needs to be strengthened with quantitative models, considering temporal variations of the relative rates of the three processes and additional complex processes, like mutual interaction of fractures due to their spatial proximity. Such modelling would provide a better understanding of the evolution of a fracture population and its size distributions in space and time.

Several workers have considered cumulative frequency in the analysis of fault or fracture length distributions (e.g., Cladouhos and Marrett 1996; Knott *et al* 1996). Such a cumulative frequency analysis of newer dolerite dikes also shows a non-power-law distribution. However, we have prefered size-class frequency (cf. Turcotte 1992; Barnsley 1993) in order to understand the nature of concentration of dikes of different lengths in the system, and their characteristic departures from a fractal trend, as shown in figure 6. In this approach it has been possible to recognize that dikes of the smallest

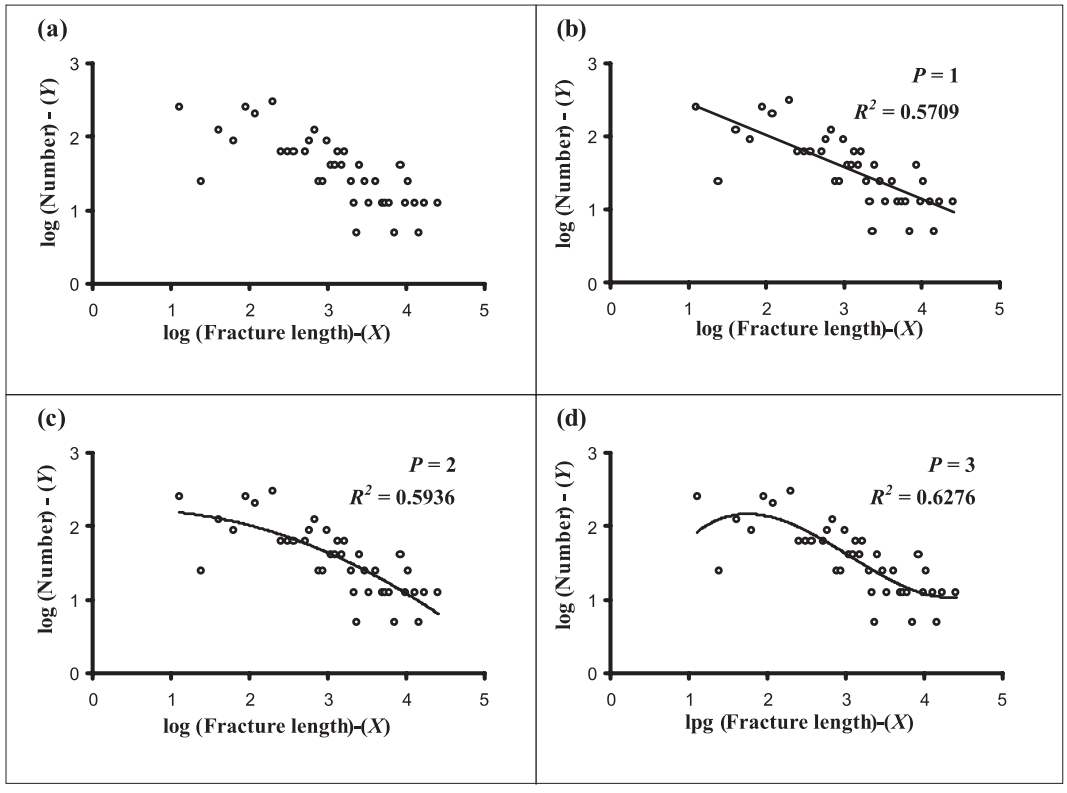

Figure 15. Analysis of fracture population in the physical model. **(a)** Plot (logarithmic) of fracture lengths versus their corresponding numbers. **(b)–(d)** Extrapolation of the best fitting curve to the data by increasing polynomial degree (P).

and largest sizes show departures from a probable fractal trend.

Geochronological studies reveal that the newer dolerite dikes were emplaced in the Singhbhum Craton over a broad time span, K–Ar dates for the dikes range from 923 Ma to 2144 Ma (Mukhopadhyay 2001). Their present topology is evidently a result of the progressive history of fracturing, as observed in physical model experiments. To analyze a fracture population we primarily need to know whether fractures forming the population belong to a system, and developed in the same stress field. They may form in the system sequentially at different stages, and show different ages in geological time scale. It appears from the consistent geometrical dispositions that dikes in the Singhbhum Craton have evolved in the same tectonic stress field.

Natural fracture systems have been studied in physical experiments. Both natural and experimental fractures show grossly similar size-distributions in log space, which are characterized by a polynomial function with degrees higher than 2. However, further experiments are required to test whether shear fractures in experimental conditions exhibit similar distributions. It may be noted that large-scale failure by shear fracturing generally follows the Coulomb–Navier criterion. On the other hand, extensional fractures that we simulated in brittle layers have probably developed following Griffith's failure criterion. Experiments are thus required to verify whether the size distribution of a fracture population can be dependent on the failure criterion.

In this study we have described newer dolerite dikes of the Singhbhum Craton as bodies emplaced along shear fractures. The prime focus of our analysis, however, is not concerned with the mechanics of dike emplacement, which can take place in different ways, e.g., hydrofracturing, faulting and tensile fracturing (Anderson 1936; Pollard 1973; Spence and Turcotte 1985; Pollard and Segall 1987; Gudmundsson 1990; Parker *et al* 1990; Gautneb and Gudmundsson 1992; Gudmundsson 1995; Fialko and Rubin 1999; Gudmundsson 2002). The bases of designating the dikes as shear fractures are as follows:

- They occur in two distinct conjugate sets on varying scales, as commonly observed in case of shear fractures produced under triaxial tests of brittle materials.
- The two sets broadly show a similar spectrum of geological age.
- The conjugate orientations are consistent with an overall N–S tectonic compression in the

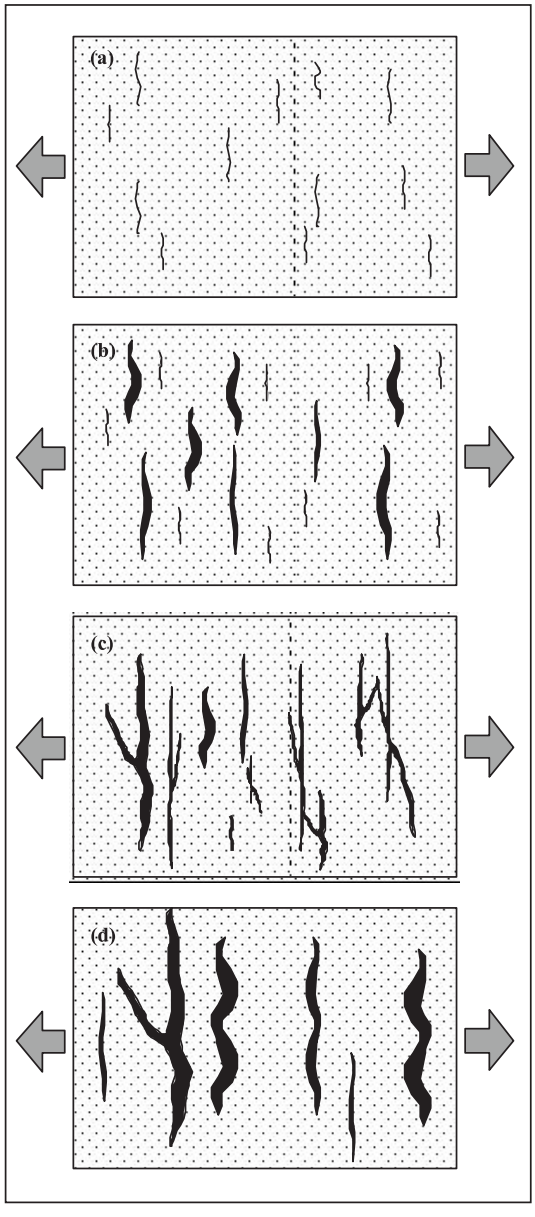

Figure 16. A schematic sketch demonstrating nucleation of fractures and their subsequent propagation and coalescence in the course of model deformation.

craton. Individual dikes often run for tens of kilometres, implying a large-scale failure in the system. It is a well-established fact that the uppermost crust on a large scale behaves essentially like a Coulomb material, and fails through shear fractures following Coulomb–Navier criterion. This is the reason why scaled experiments on large-scale faults are performed using Coulomb materials, such as non-cohesive sand (McClay and Ellis 1987).

- Most of the dikes are nearly vertical, and contain slickensides, implying shearing movement along them.
- These are similar to many Proterozoic dike swarms of fault origin (Windley 1982).

Our analysis considers the outcrop traces of dikes as one-dimensional object, and analyzes the distribution of their length dimensions without any connotation to their spatial density. It has been possible to follow this method, as the dikes describe simple, linear geometry, and do not show much irregularity in their trajectories, as often observed in many natural features, like dendritic streams or coastlines. Evidently, alternative methods would be required to handle such complex geometrical systems. For example, one can employ a method like the Box-counting method. The basic operation in this method involves overlaying a grid of square boxes over the object under consideration, and counting the number of boxes (N_n) as a function of their size (r_n). It can be shown that a system containing objects with fractal distributions will have a linear relation between N_n and r_n in log–log plot. However, special computer software is required in order to employ such a method.

7. Conclusions

The principal outcomes of our analysis are as follows.

- Newer dolerite dikes of the Singhbhum Craton grossly show a non-power-law size distribution.
- NW–SE ($n = 401$) and NE–SW ($n = 948$) trending dikes have more or less similar size distribution patterns, which are characterized by a non-linear variation in the log space. Sigmoidal curves representing the variation are typical, which is also observed in physical experiments.
- A polynomial function with degree 3–4 fits with the non-linear variation.
- Complex fracture-size distributions result due to the nature of fracture development, which involve three processes: nucleation, propagation and coalescence at varying relative rates in the course of evolution of a fracture population.
- The overall two sets of dikes in the Singhbhum Craton show dispersions from the mean trend in their orientation, which tend to reduce with increasing length. The angular deviations from the mean orientation show an inverse relation with dike length, and the relation is found to be non-linear in both arithmetic and log space.

Acknowledgements

We thank two anonymous reviewers and Dr. A Gudmundsson for their thorough and constructive reviews. We are grateful to

Prof. S C Sarkar for fruitful discussions on the geological map of Singhbhum Craton. Financial support from the CSIR, India and DST, India is greatly appreciated. CC acknowledges the infrastructural facilities provided by the Indian Statistical Institute, Kolkata.

References

Ackermann R V, Schlische R W and Withjack M O 2001 The geometric and statistical evolution of normal fault systems: an experimental study of the effects of mechanical layer thickness on scaling laws; *J. Struct. Geol.* **23** 1803–1819.

Anderson E M 1936 Dynamics of formation of cone-sheets, ring dykes and cauldron subsidence; *Proc. Royal Soc. Edinburgh* **56** 128–163.

Atkinson B K 1987 Introduction to fracture mechanics and its geophysical applications. In: Fracture Mechanics of Rock (ed.) Atkinson B, (London: Academic Press) pp. 1–26.

Barnsley M F 1993 Fractals Everywhere (2nd edn.) (San Francisco: Morgan Kaufmann).

Basu S 1996 Fracture populations in compressional and tensile stress regimes: an experimental study; M.Sc thesis (unpublished) Jadavpur University.

Cello G 1997 Fractal analysis of a Quaternary fault array in the central Apennines, Italy; *J. Struct. Geol.* **19** 945–953.

Cladouhos T T and Marrett R 1996 Are fault growth and linkage models consistent with power-law distributions of fault lengths?; *J. Struct. Geol.* **18** 281–293.

Clark R M and Cox S J D 1996 A modern regression approach to determining fault displacement-length scaling relationships; *J. Struct. Geol.* **18** 147–152.

Cowie P A and Scholz C H 1992 Displacement-length scaling relationship for faults: data synthesis and discussion; *J. Struct. Geol.* **14** 1149–1156.

Cowie P A, Vanneste C and Sornette D 1993 Statistical physical model for the spatio-temporal evolution of faults; *J. Geophys. Res.* **98** 21,809–21,821.

Dunn J A 1929 The Geology of North Singhbhum including parts of Ranchi and Manbhum Districts; *Geol. Surv. India Memoir*, Vol. LIV.

Dunn A J, Dey A K 1942 The geology and petrology of Eastern Singhbhum and surrounding areas; *Geol. Surv. India Memoir*, Vol. LXIX, Part-2.

Fialko Y A and Rubin A M 1999 Thermal and mechanical aspects of magma emplacement in giant dike swarms; *J. Geophys. Res.* **104** 23,033–23,049.

Griggs D T and Handin J 1960 Observations on fracture and a hypothesis of earthquakes; In: Rock Deformation (a symposium) (eds) Griggs D T and Handin J, *Geol. Soc. America Memoir* **79** 347–364.

Gross M R, Alonso G G, Bai T, Wacker M A, Collinsworth K B and Behl R 1997 Influence of mechanical stratigraphy and kinematics on fault scaling relations; *J. Struct. Geol.* **19** 171–183.

Gautneb H and Gudmundsson A 1992 Effect of local and regional stress fileds on sheet emplacements in west Iceland; *J. Volcanol. Geotherm. Res.* **51** 339–356.

Gudmundsson A 1990 Emplacement of dikes, sills and crustal magma chambers at divergent plate boundaries; *Tectonophys.* **176** 257–275.

Gudmundsson A 1995 Internal structure and mechanics of volcanic systems in Iceland; *J. Volcanol. Geotherm. Res.* **64** 1–22.

Gudmundsson A 2000 Fracture dimensions, displacements and fluid transport; *J. Struct. Geol.* **22** 1221–1231.

Gudmundsson A 2002 Emplacement and arrest of sheets and dykes in central volcanoes; *J. Volcanol. Geotherm. Res.* **116** 279–298.

Gudmundsson A 2004 Effects of mechanical layering on the development of normal faults and dikes in Iceland; *Geodinamica Acta* **18** 11–30.

Gupta A and Basu A 2000 North Singhbhum Proterozoic Mobile Belt, Eastern India – a review; *Geol. Surv. India Spec. Publ.* **No. 55** 195–226.

Jackson P and Sanderson D J 1992 Scaling of fault displacements from the Badajoz-Corborda shear zone, NW Spain; *Tectonophys.* **210** 179–190. Applications. (London: Chapman and Hall Ltd.).

Jager J C 1969 Elasticity, Fracture & Flow (London: Methuen and Co Ltd).

Ji S, Zhao P and Saruwatari K 1997 Fracturing of Garnet crystals in anisotropic rocks during uplift; *J. Struct. Geol.* **19** 603–620.

Klausen M B 2004 Geometry and mode of emplacement of the Thverartindur cone sheet swarm, SE Iceland; *J. Volcanol. Geotherm. Res.* **138** 185–204.

Korvin G 1992 Fractal Models in the Earth Sciences (Amsterdam: Elsevier), p. 396.

Li V C 1987 Mechanics of shear rupture applied to earthquake zones; In: Fracture Mechanics of Rock, (ed.) Atkinson B K (London: Academic Press) pp. 351–428.

Knott S D, Beach A, Brockbank P J, Lawson Brown J, McCallum J E and Welbon A I 1996 Spatial and mechanical controls on normal fault populations; *J. Struct. Geol.* **18** 359–372.

McClay K R and Ellis P G 1987 Geometries of extensional fault systems developed in model experiments; *Geology* **15** 341–344.

Marett R A and Allmendinger R W 1991 Estimates of strain due to brittle faulting: sampling of fault populations; *J. Struct. Geol.* **13** 735–738.

Mandal N, Deb S K and Khan D 1994 Evidence for a nonlinear relationship fracture spacing and layer thickness; *J. Struct. Geol.* **16** 1275–1281.

Mandal N, Chakraborty C and Samanta S K 2000 Boudinage in multilayered rocks under layer-normal compression; *J. Struct. Geol.* **22** 373–382.

Mandelbrot B B 1967 How long is the coastline of Britain? Statistical self-similarity and fractional dimension; *Science* **156** 636–638.

Mukhopadhayay D 2001 The Arachean Nucleus of Singhbhum: The Present State of Knowledge; *Gondwana Res.* **4** 307–318.

Nicol A, Walsh J J, Watterson J and Gillespie P A 1996 Fault size distribution – are they really power-law?; *J. Struct. Geol.* **18** 191–197.

Parker A J, Rickwood P C and Tucker D H (eds.) 1990 Mafic Dykes and Emplacement Mechanisms (Rotterdam: Balkema).

Paterson M S 1978 Experimental rock deformation. The Brittle Field (New York: Springer-Verlag).

Pollard D D 1973 Derivation and evaluation of a mechanical model for sheet emplacement; *Tectonophys.* **19** 233–269.

Pollard D D and Segall P 1987 Theoretical displacements and stresses near fractures in rocks: with application to faults, joints, veins, dikes and solution surfaces; In: Fracture Mechanics of Rock, (ed.) Atkinson B K (London: Academic Press) pp. 277–349.

Poulimenos G 2000 Scaling properties of normal fault populations in the western Corinth Graben, Greece:

implications for fault growth in large strain settings; *J. Struct. Geol.* **22** 307–322.

Ranalli G 1987 Rheology of the Earth (Boston: Allen & Unwin).

Saha A K 1994 Crustal Evolution of Singhbhum-North Orrisa, Eastern India; *Geol. Soc. India, Bangalore. Memoir* **27**.

Sarkar S N and Saha A K 1962 A revision of the Precambrian stratigraphy and tectonics of Singhbhum and adjacent regions; *Q. J. Geol. Min. Metall. Soc. India* **34** 97–136.

Sarkar S C 1984 Geology and ore mineralisation of the Singhbhum Copper Uranium belt, Eastern India (Calcutta: Jadavpur Univ. Publ.).

Spence D A and Turcotte D L 1985 Magma-driven propagation of cracks; *J. Geophys. Res.* **90** 575–580.

Turcotte D L 1992 Fractals and Chaos in Geology and Geophysics; (Cambridge: Cambridge University Press).

Van Dijk J P, Bello M, Toscano C, Bersani A and Nardon S 2000 Tectonic model and three-dimensional fracture network analysis of Monte Alpi (southern Apennines); *Tectonophys.* **324** 203–237.

Vermilye J and Scholz C H 1995 Relation between vein length and aperture; *J. Struct. Geol.* **17** 423–434.

Villemin T, Angelier J and Sunwoo C 1995 Fractal distribution of fault length and offsets: implications of brittle deformation evaluation – the Lorraine Coal Basin; In: *Fractals in the Earth Sciences* (eds) Barton C C and La Pointe P R, (New York: Plenum Press).

Volland S and Kruhl J K 2004 Anisotropy quantification: the applicaton of fractal geometry methods on tectonic fracture patterns of a Hercynian fault zone in NW Sardinia; *J. Struct. Geol.* **26** 1499–1510.

Walsh J J and Watterson J 1992 Populations of faults and fault displacements and their effects on estimates of fault-related regional extension; *J. Struct. Geol.* **14** 701–712.

Walsh J J, Watterson J and Yielding G 1991 The importance of small-scale faulting in regional extension; *Nature* **351** 391–393.

Watterson J, Walsh J J, Gillespie P A and Easton S 1996 Scaling systematics of fault sizes on a large-scale range fault map; *J. Struct. Geol.* **18** 199–214.

Windley B F 1982 The Evolving Continents (2nd edn) (London: John Wiley & Sons).

Wojtal S F 1996 Changes in fault displacement populations correlated to linkage between faults; *J. Struct. Geol.* **18** 265–279.

Yielding G, Needham T and Jones H 1996 Sampling of fault populations using sub-surface data: a review; *J. Struct. Geol.* **18** 135–146.

MS received 21 July 2005; revised 26 April 2006; accepted 5 June 2006